

AIAA 80-1097R

# Experiments of Surface Tension Separator for Propellant Feed System

S. Enya,\* T. Kisaragi,† J. Ochiai,‡ and Y. Sasao‡

*Ishikawajima-Harima Heavy Industries Co., Ltd., Tokyo, Japan*

and

K. Kuriki§

*Institute of Space and Aeronautical Science, University of Tokyo, Tokyo, Japan*

The effects of surface tension on propellant confinement in the feed tank of a plasma thruster, MPD arcjet were experimentally investigated under high acceleration. Ethanol and ammonia were used in the fundamental experiments so as to decide the kind of material and the specifications of the tank. The relationships between the sustained liquid height and the capillary diameter were examined under various conditions. On the basis of these data, the model of the propellant feed system was designed. Major results of ground tests were that, below 40 times Earth gravity, the liquid ammonia could be prevented from spilling out of the tank in any direction of acceleration, and that the heat input through the tank wall was large enough to vaporize the liquid. Units of an MPD arcjet with the same feed tank were installed aboard the MS-T4 satellite of the Institute of Space and Aeronautical Science, University of Tokyo. The satellite was launched on February 17, 1980, and the arcjets were successfully operated. It is possible to apply these principles to much larger systems such as space vehicles and space shuttles.

## Nomenclature

$A_0$	= cross-sectional area of cylinder
$a$	= $\sigma_l / \rho g$
$a_e$	= $\sigma_l / \rho g_e$
$d_0$	= diameter of fiber
$g$	= acceleration
$g_e$	= acceleration by Earth gravity
$H$	= packing length
$h$	= maximum liquid height
$L$	= latent heat for vaporization
$\ell$	= length immersed into liquid
$\ell_t$	= total length of fiber
$r_c$	= capillary radius
$r_0$	= radius of fiber
$r_{eq}$	= equivalent radius of capillary
$T_s$	= saturation temperature
$\Delta T_s$	= superheat for boiling
$t$	= time
$u$	= terminal velocity
$v$	= specific volume
$W$	= sustained weight
$W_0$	= initially filled weight
$\alpha$	= porosity
$\theta$	= contact angle
$\kappa$	= permeability
$\nu$	= kinematic viscosity
$\rho$	= liquid density
$\sigma$	= surface tension

## Subscripts

$l$	= liquid
$s$	= solid
$v$	= vapor
$lv$	= interface between liquid and vapor

## Introduction

UNDER the circumstances of microgravity or  $g$ -jitter, vapor cannot be easily separated from the liquid propellant feed as is done under Earth gravity. Various systems have been used for vapor separation.

One is to arrange a shut-off valve at the outlet of the tank so that it can open only when the feed is required, and the relieved liquid be heated and vaporized. Other systems may involve a mechanical centrifugal system, a dielectrophoretic control system, and so on. All of these methods need, however, both extra energy and equipment for operation.

In contrast, a surface tension separator can prevent the liquid from flowing out of the storage tank if it is packed in appropriate capillaries. In short, this system has the following advantages:

- 1) It does not need any peripheral equipment or energy.
- 2) The design can be made very compact.

In designing the evaporator tank with capillary confinement and integrating it in the feed system of space vehicles or satellites, the following information was required:

- 1) The relation of the sustained liquid height to the capillary diameter and porosity.
- 2) The effect of wettability (or contact angle) on liquid behavior.
- 3) Evaporation characteristics (especially with respect to the entrainment of liquid drops or particles out of porous material).

Theoretical equations were solved as an ideal system in a recent research development.<sup>1</sup> The material in practical use, however, has some negative influence such as contamination and adsorption on surface energy. So, experimental data should be obtained with actual construction and material. To establish a reliable design basis, some fundamental experiments were made using ethanol and ammonia.

A surface tension type of zero- $g$  reservoir was developed for an ion microthruster system and operated successfully for the satellite (ATS)-IV.<sup>2,3</sup> The reservoir consisted of a cylindrical volume enclosing a fin array (120 fins). The propellant was stably sustained with surface tension force in the area between fins. As a previous work for this ATS-IV development, the reservoir with porous metal was designed to be operated in a  $1-g_e$  field, and also a vaporizer heater with capillary tubes was considered to remove the liquid toward the engine.<sup>4</sup>

Presented as Paper 80-1097 at the AIAA/SAE/ASME 16th Joint Propulsion Conference, Hartford, Conn., June 30-July 2, 1980; submitted Aug. 25, 1980; revision received March 31, 1981. Copyright © American Institute of Aeronautics and Astronautics, Inc., 1980. All rights reserved.

\*Chief Research Engineer, Research Institute. Member AIAA.

†Research Engineer, Research Institute.

‡Senior Manager, Space Development Division.

§Associate Professor. Member AIAA.

The space shuttle reaction system (RCS) also had a surface tension acquisition tank. RCS is required to supply gas-free propellant during the low- and high- $g$  operational environment ( $3.3g_e$ ).<sup>5,6</sup> A fine-mesh screen was used for the surface tension device. RCS and the screen supply the engine or the vaporizer with the liquid feed.

In this MPD-thruster system, the requirement was unique. The tank without a shut-off valve and a vaporizer at the outlet had to store the liquid to supply liquid-free propellant vapor intermittently during the low- and high- $g$  environment ( $40g_e$ ). Therefore, the fine capillaries should be used to confine the propellant.

Other studies have also been done on the behavior of the liquid enclosed in the tank. In this paper, the tank is designed such that the liquid might not flow along the wall based on earlier work.<sup>7,8</sup>

Evaporating liquid has an incipient boiling superheat on a surface with cavities. Capillaries could be possible nucleation sites. Thus, if boiling occurs in the tank, some disadvantages such as entrainment of droplets, vapor-locking, etc., exist.

The heat of vaporization may be conducted through the tank packing material and the cell wall and is primarily dependent on the structural design of the tank. In order to demonstrate performance, a model was fabricated and tested.

## Fundamental Investigations

### Material Wettability

A surface tension separator for a space propellant feed system confines the liquid in the capillary. This enables one to make the structure simpler with no other equipment or energy except porous material, and the tank can be made very compact. It is important to know the behavior of the propellant in the porous matrix for each system.

First, wettability between the liquid and the porous medium was investigated. Wettability is established by the contact angle between the solid surface and the liquid. When contact angles ( $\theta$ ) on a solid surface were measured by using various liquids having the surface tension ( $\sigma_l$ ) and  $\cos\theta$  for an ordinate vs  $\sigma_l$  for an abscissa was plotted, the almost linear relations in each solid was obtained as shown in Fig. 1. The critical surface tension is defined as the surface tension at the point where the above-mentioned line cuts the line:  $\cos\theta = 1$ . If the surface tension is less than the critical surface tension, the liquid spreads on the solid surface.

Zisman studied experimentally the wettability of many solid materials and concluded the following<sup>9-12</sup>:

- 1) Low-free-energy surfaces have smaller critical surface tensions and some organic liquids having larger surface tension than the critical surface tension could not spread on polymers, waxes, or covalent compounds.
- 2) High-free-energy surfaces have larger critical surface tensions and all liquids should spread on most metals and other inorganic high melting solids if their surfaces are clean and specularly smooth.

- 3) High-energy surfaces, however, have larger adsorption forces. If the surface is not free from organic contamination, the film adsorbed by the solid is so constituted that the resulting film-coated surface is a low-energy surface even if the film is monomolecular layer, and nonspreading occurs.

The experimental results of polytetrafluorethylene (PTFE) and polyethylene are plotted in Fig. 1.<sup>9,10</sup> Surface tension generally decreases with rising temperature and the liquid does not spread at lower temperature, even though it could spread at higher temperature on the same surfaces. For example, surface tensions of  $\text{NH}_3$  are shown at three different temperatures on the horizontal axis of Fig. 1. Those materials that cannot be used as a capillary matrix, can be used preferably as the structure or baffle in the vessel.

Experimental data for solids such as glass, quartz, sapphire, stainless steel, gold, silver, and other metals are shown by the dotted line:  $\cos\theta = 1$ .<sup>11,13,14</sup>

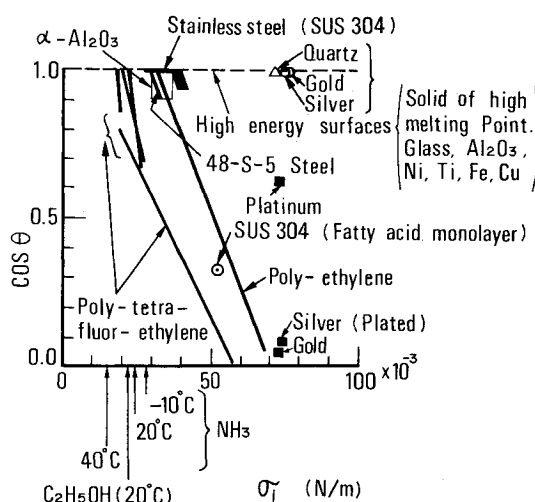


Fig. 1 Relation between contact angle and surface tension.<sup>9-15</sup>

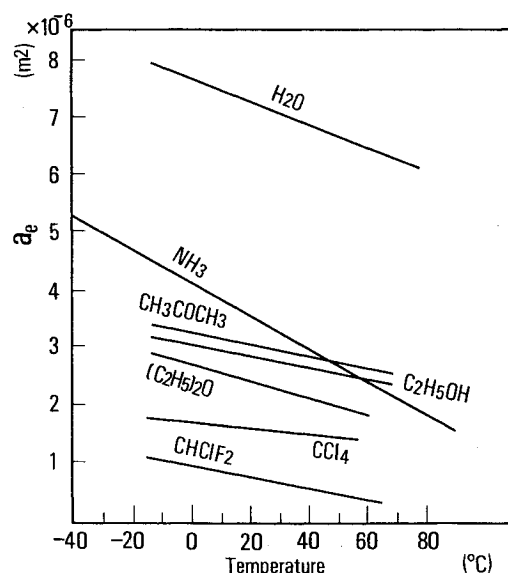


Fig. 2 Comparison of  $\sigma_c$  for several liquids.

Zisman described the cleaning procedures for stainless steel. He stated that no cleaning technique involving solvents—including the Bureau of Aeronautics specification method—was completely satisfactory. The only acceptable method involved polishing the stainless steel on a cloth lap with an aqueous slurry of  $\gamma\text{-Al}_2\text{O}_3$ ; the powder of  $\text{Al}_2\text{O}_3$  was removed on a second lap wet with distilled water, then the specimen was rinsed in hot freshly distilled water and dried in a clean oven at  $110^\circ\text{C}$ .<sup>11</sup> Some data for stainless steel and noble metals which were not free from contamination are shown in Fig. 1.<sup>12,15</sup> Several data of other steel and sapphire show that contact angles do not seem to be zero around  $\sigma_l = 0.03 \text{ N/m}$ .<sup>11,13</sup> Thus, stainless-steel fiber seems to be difficult to clean once its surface is contaminated. Stainless-steel fiber in commercial use (Naslon) was not wettable against water and ethanol. Those results and compatibility with  $\text{NH}_3$  suggest that glass fiber, quartz fiber, and ceramic fiber are better for practical use.

### Predictions of Sustained Liquid Height

In the case where capillaries are arranged in the same direction as acceleration, the following equation can be derived for the maximum hydrostatic head supportable under

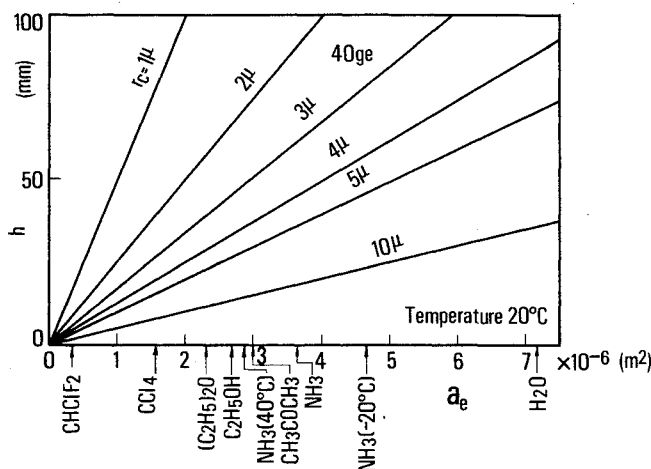


Fig. 3 Predicted liquid height in a capillary under  $40g_e$ .

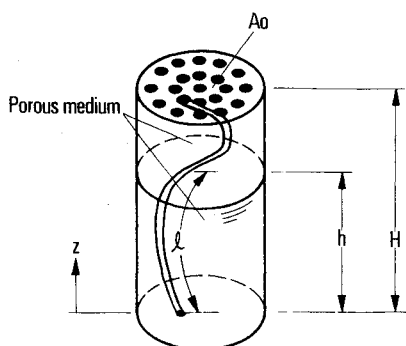


Fig. 4 Sketch showing the cylindrical tank packed with porous medium partially filled with propellant.

no-flow conditions:

$$h = \frac{2\sigma_l \cos\theta}{\rho g r_c} = 2a \frac{\cos\theta}{r_c} \quad (1)$$

Sustained height is proportional to  $a$  divided by the constant  $r_c$ . The values of  $a$  for various liquid under Earth gravity ( $g_e$ ),  $a_e = \sigma_l / \rho g_e$ , are shown in Fig. 2. The physical properties are given in Refs. 16 and 17. The values of acetone and ethanol are similar to the value of ammonia.

If the surface wettability is large enough,  $\theta$  is zero, and then the maximum sustained heights ( $h$ ) are calculated with Eq. (1) under 40 Earth gravities and are shown with  $r_c$  as the parameter and  $a_e$  for the abscissa in Fig. 3. The limit of the radius for the design is derived from the figure. For example, if 25 mm is required for  $h$  with ethanol, the radius should be  $5 \mu\text{m}$ .

In ordinary fibrous layers, channel space and direction of fiber are not uniform. If porosity and the diameter of fiber are known, however, total surface areas are obtained and the liquid height can be calculated under the condition of minimum energy of the system.<sup>1</sup> The model is shown in Fig. 4. Assuming that the tank is a circular cylinder, total energy is expressed by the following equation:

$$E(h) = \rho g \int_0^h \alpha A_0 z dz + 2\pi r_0 (\ell_l - \ell) \sigma_{sv} + 2\pi r_0 \ell \sigma_{sl} + A_0 \sigma_{lv} \quad (2)$$

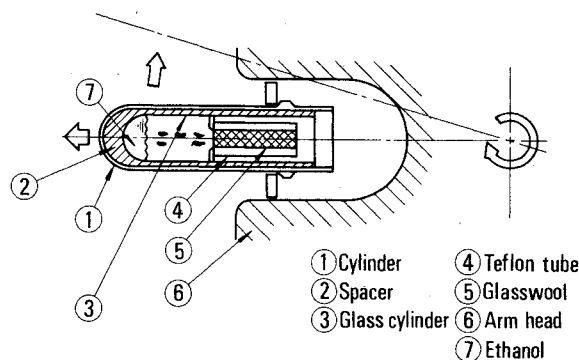


Fig. 5 Open-type capsule for ethanol.

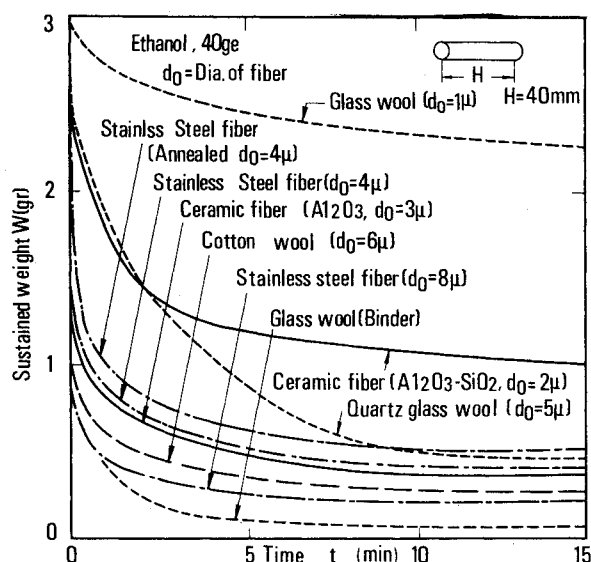


Fig. 6 Experimental results with ethanol for various fibers.

From  $dE(h)/dh = 0$  and Young's relation,  $h$  is obtained.

$$h = \frac{2\pi r_0 \ell_l \sigma_l \cos\theta}{\rho g \alpha A_0 H}$$

and as  $\ell_l/H$  is replaced by  $(1 - \alpha) A_0 / \pi r_0^2$ ,

$$h = 2a \frac{\cos\theta}{\alpha r_0 / 1 - \alpha} = 2a \frac{\cos\theta}{r_{eq}} \quad (3)$$

$$r_{eq} = \frac{\alpha}{1 - \alpha} r_0 \quad (4)$$

If  $r_0 = 0.5 \mu\text{m}$  and  $r_{eq} = 5 \mu\text{m}$ , then,  $\alpha = 0.9$  results.

### Fundamental Experiments

Experiments with ethanol were made to compare with the above calculations. Fibers of several different materials were tested. They were packed with a porosity of about 0.95 after cleaning. The capsule used for the test is shown in Fig. 5. The capsule was rotated by mounting on a centrifugal separator. Sustained liquid height was obtained from measuring the weight before and after rotation. If the liquid filled the capsule over the maximum weight which could be sustained under acceleration  $40 g_e$ , extra liquid fell out of the capsule in a short time and the residue was the maximum sustained weight. A small amount of liquid was lost due to evaporation into the atmosphere. The result is shown in Fig. 6.

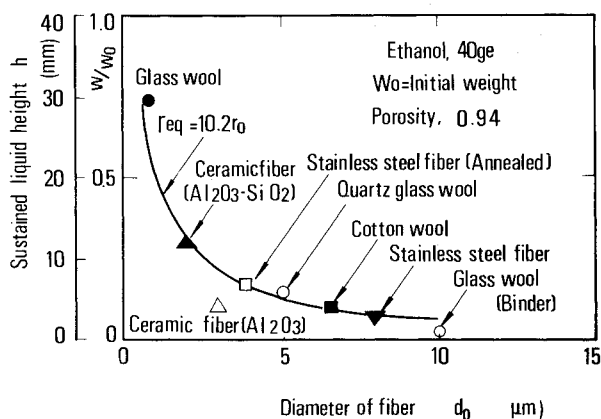
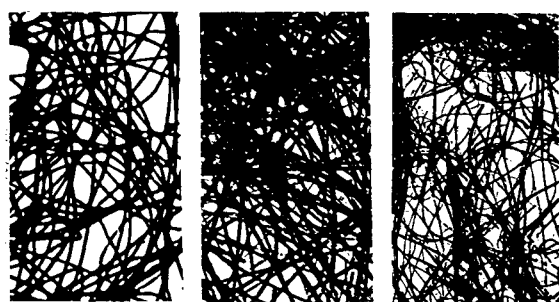


Fig. 7 Relation of sustained ethanol height to diameter of fiber.



(a) Stainless steel fiber  
(b) Quartz glass wool  
(c) Glass wool

Fig. 8 Microscopic photographs of packing fibers.

Figure 7 is a plot of liquid height against the diameter of fibers. The curve expressed by the solid line in the figure is similar to the values calculated by Eq. (3) when  $r_{eq}$  is equal to  $10.2r_0$  and  $\theta$  is zero, while  $r_{eq} = 15.7r_0$  by Eq. (4), when  $\alpha = 0.94$ . This shows that the sustained liquid 1.6 times as high as predicted value was obtained when compared with theoretical values. The microscopic observations ( $\times 200$ ) are shown in Fig. 8. It is apparent that the fibers are completely random. They form microchannels and the liquid is confined against gravity. This is the main reason why the liquid was sustained over the predicted height; other reasons are the uncertainties in  $\alpha$  and  $r_0$ .

Stainless-steel fiber (Naslon) was not wettable against ethanol. Therefore, the sustained height is low. Ceramic fiber (Kaowool) has good characteristics but it is found that small pieces of fiber are entrained into vapor. From Fig. 8 the ethanol height 20 mm is obtained by using fiber of  $1 \mu\text{m}$  diam.

Another experiment was made varying the length of packing glasswool. The results are shown in Figs. 9 and 10. Figure 9 is the plot of liquid weight against time. The curve for  $H = 20$  shows that a slight quantity of ethanol spills out of the capillaries a few minutes after the acceleration and the weight approximates the maximum value to be sustained. The slight decrease of this curve after equilibrium is due to the evaporation at the opening. From the inclination, the rate of evaporation was known to be around  $15 \text{ mg/min}$ . The curves for  $H = 40$  and  $H = 10$  describe the overfilled case and the underfilled case, respectively.

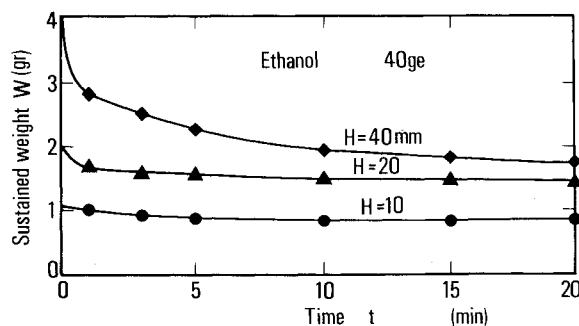


Fig. 9 Results of experiments with varied packing length.

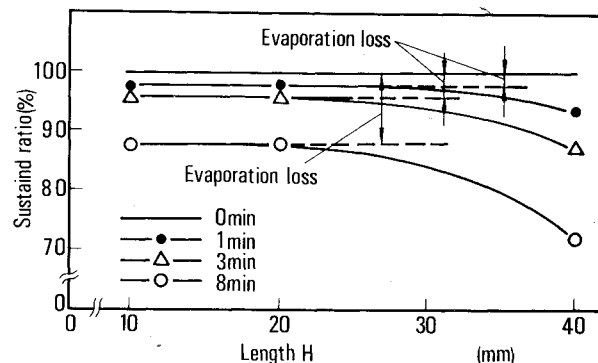


Fig. 10 Relation of sustained ratio to packing length.

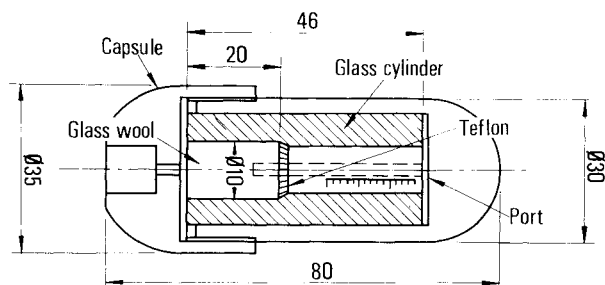


Fig. 11 Closed-type capsule for ammonia.

In every run the extra liquid was lost in the initial phase of several minutes. This is due to the delay of the flow through matrix. From the analysis of the unsteady state, the velocity in the matrix becomes

$$u = \frac{\kappa}{\nu} g (1 - e^{-(\nu/\kappa)t}) \quad (5)$$

The time constant is very short. The terminal velocity is  $4 \text{ mm/s}$  for ammonia and  $0.4 \text{ mm/s}$  for ethanol under  $40g_e$  according to this calculation. The flow takes 1 min to move through a length of 20 mm. Consequently, the curve for  $H = 40$  took some more time before reaching the equilibrium state.

Figure 10 was replotted with the same data. The curves show the portion of the sustained liquid compared with the liquid at 5 min after the acceleration exclusive of the initial loss. The result shows the maximum height under  $40g_e$  will be around 20 mm because there will be no loss except evaporation in a capsule shorter than 20 mm in length.

### Experiments with Ammonia

#### Comparison with Ethanol

Ammonia was used for the experiment to show the difference between the results obtained using ammonia and those using ethanol. The capsule is shown in Fig. 11. It was sealed hermetically after filling so that the diffusion of vapor may not occur. The length of packing glasswool was 20 mm, and

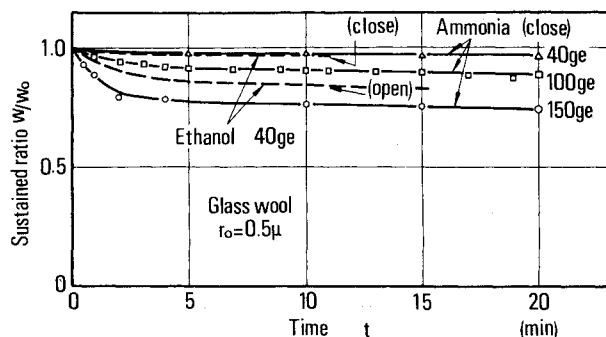


Fig. 12 Data for ammonia under various accelerations.

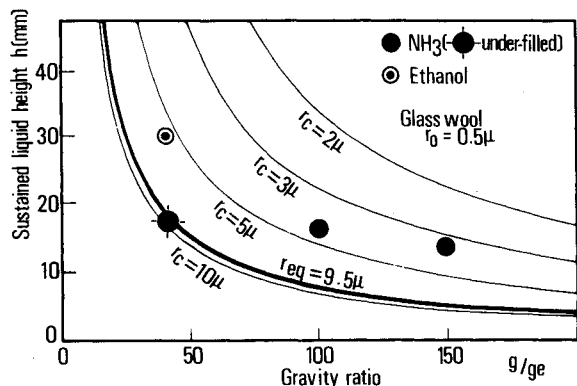


Fig. 13 Sustained ammonia height vs acceleration.

the inner diameter was 10 mm. Porosity was 0.95. Acceleration was changed from  $40g_e$  to  $150g_e$ . The volume of spread liquid was measured with the scale on the glass cylinder. A perforated baffle made of Teflon was used to prevent ammonia from spilling out or spreading out. The results are shown in Fig. 12. It is evident that no liquid spreads out under  $40g_e$ . It is also shown that liquid loss increases slowly (below 1 mg/min) for several minutes under the gravity over  $40g_e$ , and finally becomes zero. The dotted curves represent the data of ethanol, and they are of two types: open type and closed type. The open-type data are the same as those in Fig. 10. The results with ammonia are in good agreement with those of ethanol in this range of temperature. Liquid height was replotted to show its relationship to acceleration (Fig. 13). The equivalent radius of capillary was  $9.5 \mu\text{m}$ . Sustained liquid height was twice as high as the theoretical value. This is assumed to be due to the effect of perforated plate and nonuniformity of glasswool.

#### Experiments with the Model for Plasma Thruster

The model of the tank for the MPD arcjet was designed and fabricated on the basis of these data. The specifications of the thruster and the tank are given in Table 1; the model is shown in Fig. 14. The length of each cell was reduced to 10 mm, and four cells are connected in cascade to ensure separation. Thus, the tank was so designed that the liquid may not spill out in any direction when acceleration was below  $40g_e$ . The wall of the cell makes it easy to conduct heat to liquid. The total weight of the ammonia tank was 230 g, including the baffle and cells (75 g) and the packing material (1.24 g). A view port was used to watch the behavior of liquid. Evaporation was controlled by the heater attached on the tank wall, and the temperature of the surface was measured as was the vapor flow rate and feed line pressure. Vapor of ammonia passed through the flow meter and was absorbed into water.

The evaporation experiment was made at room temperature with heater off at first. Ammonia was heated by the heat flux from the tank wall with its heat capacity and was vaporized.

Table 1 Specifications of MPD thruster and ammonia tank

MPD thruster	
Propellant	NH <sub>3</sub>
Power consumption	15 W
Propellant flow rate	(max) 5 mg/s
Specific impulse	2500 s
Impulse bit	0.5 N ms
Total impulse	1000 N ms
Ammonia tank	
NH <sub>3</sub> storage weight	5 g
Temperature	260-310 K
Acceleration	0 ge-40 ge (normal) ± 5 ge (horizontal)
Tank weight	230 g
(Baffle, cells)	(75 g)
(Packing material)	(1.24 g)

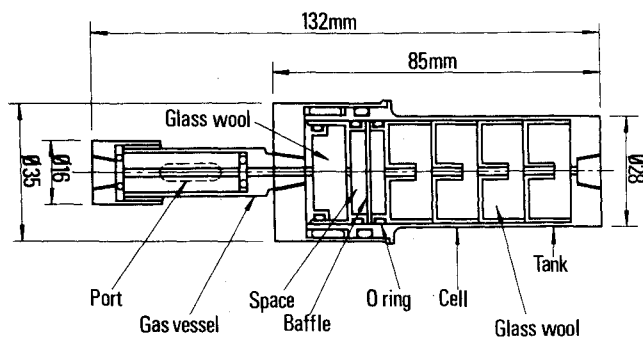


Fig. 14 Model of the tank for MPD arcjet.

The tank was cooled down in a short time, and eventually the temperature fell to the equilibrium value. The rate of evaporation became nearly zero. Second, the experiment was made at a constant wall temperature with heater on and off. The results are shown in Fig. 15. It was shown that the maximum rate for evaporation could be kept at about 1 liter/min. This value is about 100 times as high as the required rate. From this it is known that heat was conducted effectively to the liquid through the cell wall. Undesirable behavior such as vapor lock was not observed.

Superheat for incipient boiling is expressed as follows (Ref. 18):

$$\Delta T_s = 2\sigma_i T_s (v_v - v_l) / r_c L \quad (6)$$

If  $r_c = 50 \mu\text{m}$ ,  $\Delta T_s = 1 \text{ K}$ , and if  $r_c = 10 \mu\text{m}$ ,  $\Delta T_s = 5 \text{ K}$ . According to this calculation, the superheat of boiling is very large if capillary is fine as in this case. It is difficult to reach boiling.

#### Flight Test on MS-T4 Satellite

Two units of a flight model, which are the same as that used in the ground tests, were constructed and integrated in the MPD arcjet system. The arcjets were aboard the MS-T4 satellite of Institute of Space and Aeronautical Science, University of Tokyo, which was launched March 17, 1980 from Kagoshima Space Center.

From the monitor signals transmitted from the satellite, ammonia was found to be successfully confined under various accelerations and vibrations, and to supply the system with vapor. NH<sub>3</sub> vapor from the tank flowed through the filter and the valve and entered the gas reservoir to be restored. The reservoir with fast acting valve (FAV) supplied the arcjet with the gas in response to the command signal (CHG). The reservoir pressure (Pr) of FAV in MPD arcjet was regulated as follows. The valve, which controls the gas supply from the storage tank, was actuated by the command signal (JET ON) from an electronic interface unit (IU). The reservoir pressure

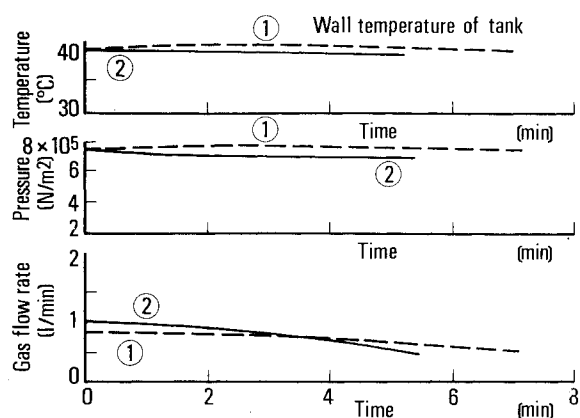


Fig. 15 Characteristics during evaporation.

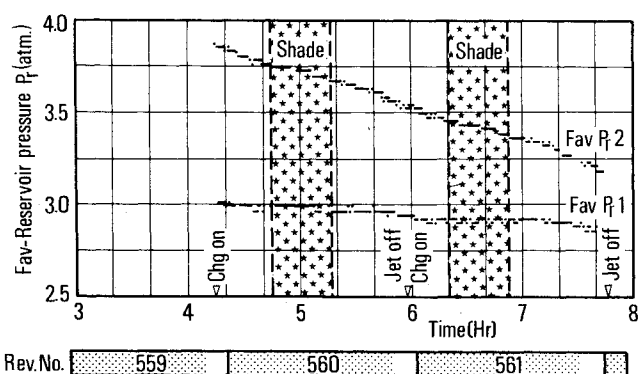


Fig. 17 History of FAV reservoir pressure during flight test on March 25, 1980.

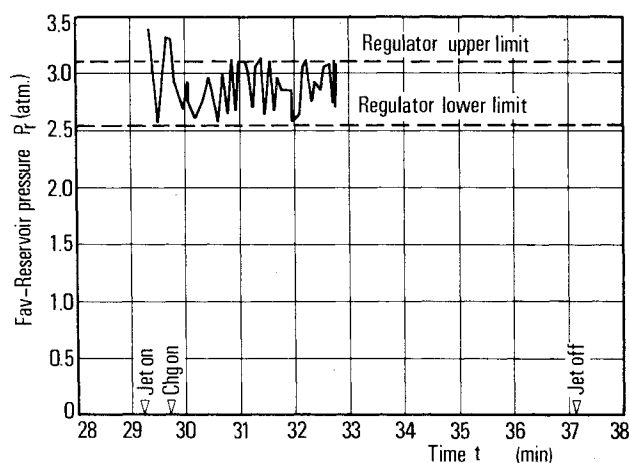


Fig. 16 Pressure regulation characteristics of thruster No. 1 during flight test on March 26, 1980.

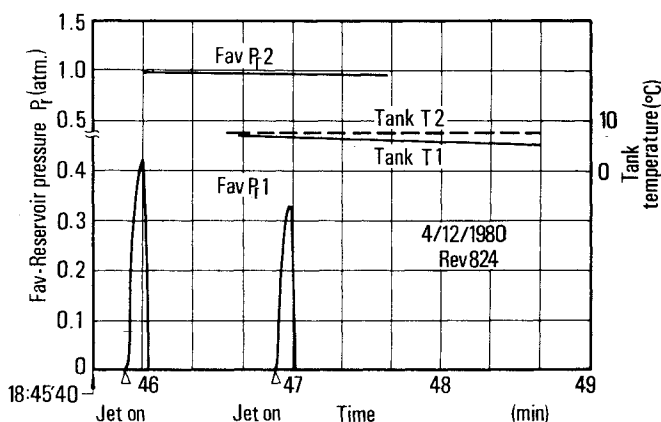


Fig. 18 Pressure change and temperature drop of thruster No. 1 during draining the vapor in the pressurized line and the reservoir on April 13, 1980.

$P_r$  was received and processed by the IU. The IU judges whether  $P_r$  is larger than a specified upper limit or less than a lower limit and sends shut-off or open command signals to the valve. This feedback loop functioned properly, as shown in Fig. 16. The FAV reservoir pressure was maintained between the two limits. The feed rate depended mainly upon the heat flow rate from the outside into the tank since the tank was controlled in a passive way.

When the arcjets were fired once every 32 s with the valve closed, the reservoir pressure of No. 2 unit decreased steadily as shown in Fig. 17. The No. 1 unit was not operated in this case and the slight decrease in  $P_r$  indicates the leakage rate of the No. 1 FAV. From the difference between the pressure reduction rate of the two units, the net propellant flow rate of No. 2 unit was found to be about 2 mg/s and to coincide with the design value. When the vapor in the pressurized line as well as the reservoir of the No. 1 unit was drained, the pressure decreased as shown in Fig. 18. The temperature drop of the No. 1 tank wall is also shown in Fig. 18. Parameters for the No. 2 unit are included for comparison.

### Conclusion

Design bases for the surface tension separator were obtained from the experiments with ethanol and ammonia. The capillary diameter must be small enough to confine the liquid against large acceleration. The materials of the fiber must be wettable for the propellant.

Sustained liquid height tends to be higher than predicted. A dry baffle was effective to prevent the liquid from spreading.

The model of the tank for plasma thruster was tested with ammonia. The liquid was sustained in the porous medium against acceleration, and no type of entrainment was observed. The required rate of evaporation was obtained.

The performance was demonstrated with the test of the tank designed and fabricated for the MPD arcjet which was launched aboard MS-T4.

### References

- Ostermeier, R.M., Nolt, I.G., and Radostits, J.V., "Capillary Confinement of Cryogenics for Refrigeration and Liquid Control in Space, I Theory," *Cryogenics*, Vol. 18, Feb. 1978, pp. 83-86.
- Warlock, R., Davis, J.J., James, E., Ramirez, P. and Wood, O., "An Advanced Contact Ion Microthruster System," *Journal of Spacecraft and Rockets*, Vol. 6, April 1969, pp. 424-429.
- Hunter, R.E. and Bartlett, R.O., "Cesium Contact Ion Microthruster Experiment Aboard Applications Technology Satellite (ATS)-IV," *Journal of Spacecraft and Rockets*, Vol. 6, Sept. 1969, pp. 968-970.
- Barcatta, F.A., Forrester, A.T., and Trump, G.E., "Propellant Systems for Ion Engines," AIAA Paper 66-249, March 1966.
- Fester, D.A., Eberhardt, R.N., and Tegart, J.R., "Space Shuttle Reaction Control System Propellant Acquisition Technology," *Journal of Spacecraft and Rockets*, Vol. 12, Dec. 1975, pp. 705-710.
- Fester, D.A., Villars, A.J., and Uney, P.E., "Surface Tension Propellant Acquisition System Technology for Space Shuttle Reaction Control Tanks," *Journal of Spacecraft and Rockets*, Vol. 13, Sept. 1976, pp. 522-527.
- Gluck, D.F. and Gille, J.P., "Fluid Mechanics of Zero-g Propellant Transfer in Spacecraft Propulsion Systems," *Journal of Engineering for Industry*, Vol. 87, Feb. 1965, pp. 1-8.
- Gluck, D.F., "Propellant Position Control by Capillary Barriers during Spacecraft Rotational Maneuvers," *Journal of Spacecraft and Rockets*, Vol. 7, March 1970, pp. 242-247.

<sup>9</sup>Fox, H.W. and Zisman, W.A., "The Spreading of Liquids on Low Energy Surfaces," *Journal of Colloid Science*, Vol. 5, Dec. 1950, pp. 514-531.

<sup>10</sup>Ellison, A.H. and Zisman, W.A., "Wettability of Halogenated Organic Solid Surfaces," *Journal of Physical Chemistry*, Vol. 58, March 1954, pp. 260-265.

<sup>11</sup>Fox, H.W., Hare, E.F., and Zisman, W.A., "Wetting Properties of Organic Liquids on High Energy Surfaces," *Journal of Physical Chemistry*, Vol. 59, Oct. 1955, pp. 1097-1106.

<sup>12</sup>Cottigton, R.L., Shafrin, E.G., and Zisman, W.A., "Physical Properties of Monolayers at the Solid/Air Interface III," *Journal of Physical Chemistry*, Vol. 62, May 1958, pp. 513-518.

<sup>13</sup>Miller, N.F., "The Wetting of Steel Surfaces by Esters of Unsaturated Fatty Acids," *Journal of Physical Chemistry*, Vol. 50, July 1946, pp. 300-319.

<sup>14</sup>Bartell, F.E. and Smith, J.T., "Alteration of Surface Properties of Gold and Silver as Indicated by Contact Angle Measurement," *Journal of Physical Chemistry*, Vol. 57, Feb. 1953, pp. 165-172.

<sup>15</sup>Erb, R.A., "Wettability of Metals under Continuous Condensing Conditions," *Journal of Physical Chemistry*, Vol. 69, April 1965, pp. 1306-1309.

<sup>16</sup>Touloukian, Y.S., *Tables on the Thermophysical Properties of Liquids and Gases*, Hemisphere Publishing Corporation, 1975.

<sup>17</sup>Stairs, R.A. and Sienko, M.T., "Surface Tension of Ammonia and of Solutions of Alkali Halides in Ammonia," *Journal of American Chemical Society*, Vol. 78, March 1956, pp. 920-923.

<sup>18</sup>Rohsenow, W.M., "Nucleation with Boiling Heat Transfer," ASME Paper, 70-HT-18, 1970.

*From the AIAA Progress in Astronautics and Aeronautics Series..*

## AERODYNAMIC HEATING AND THERMAL PROTECTION SYSTEMS—v. 59 HEAT TRANSFER AND THERMAL CONTROL SYSTEMS—v. 60

*Edited by Leroy S. Fletcher, University of Virginia*

The science and technology of heat transfer constitute an established and well-formed discipline. Although one would expect relatively little change in the heat transfer field in view of its apparent maturity, it so happens that new developments are taking place rapidly in certain branches of heat transfer as a result of the demands of rocket and spacecraft design. The established "textbook" theories of radiation, convection, and conduction simply do not encompass the understanding required to deal with the advanced problems raised by rocket and spacecraft conditions. Moreover, research engineers concerned with such problems have discovered that it is necessary to clarify some fundamental processes in the physics of matter and radiation before acceptable technological solutions can be produced. As a result, these advanced topics in heat transfer have been given a new name in order to characterize both the fundamental science involved and the quantitative nature of the investigation. The name is Thermophysics. Any heat transfer engineer who wishes to be able to cope with advanced problems in heat transfer, in radiation, in convection, or in conduction, whether for spacecraft design or for any other technical purpose, must acquire some knowledge of this new field.

Volume 59 and Volume 60 of the Series offer a coordinated series of original papers representing some of the latest developments in the field. In Volume 59, the topics covered are 1) The Aerothermal Environment, particularly aerodynamic heating combined with radiation exchange and chemical reaction; 2) Plume Radiation, with special reference to the emissions characteristic of the jet components; and 3) Thermal Protection Systems, especially for intense heating conditions. Volume 60 is concerned with: 1) Heat Pipes, a widely used but rather intricate means for internal temperature control; 2) Heat Transfer, especially in complex situations; and 3) Thermal Control Systems, a description of sophisticated systems designed to control the flow of heat within a vehicle so as to maintain a specified temperature environment.

*Volume 59—432 pp., 6 × 9, illus. \$20.00 Mem. \$35.00 List*

*Volume 60—398 pp., 6 × 9, illus. \$20.00 Mem. \$35.00 List*

TO ORDER WRITE: Publications Dept., AIAA, 1290 Avenue of the Americas, New York, N.Y. 10019